Capicua suppresses hepatocellular carcinoma progression by controlling ETV4-MMP1 axis

Eunjeong Kim[1], Donghyo Kim[1], Jeon-Soo Lee[1], Jeehyun Yoe[1], Jongmin Park[1], Chang-Jin Kim[3], Dongjun Jeong[3,4], Sanguk Kim[1,2,*], and Yoontae Lee[1,2,*]

e-mail addresses of authors (in the order of listed authors)

eunjeongkim@postech.ac.kr, kimdh4962@postech.ac.kr, luceinaltis@postech.ac.kr, jhyoe@postech.ac.kr, jongmin@postech.ac.kr, cjkim@sch.ac.kr, juny1024@sch.ac.kr, sukim@postech.ac.kr, yoontael@postech.ac.kr

[1]Department of Life Sciences, [2]Division of Integrative Bioscience and Biotechnology, Pohang University of Science and Technology, Pohang, Gyeongbuk, Republic of Korea

[3]Department of Pathology, [4]Soonchunhyang Medical Science Research Institute, College of Medicine, Soonchunhyang University, Cheonan, Chungnam, Republic of Korea

2

*Corresponding authors

Sanguk Kim, Room 103, Life Science Building, 77 Cheongam-Ro, Nam-Gu, Pohang,

Gyeongbuk 37673, Republic of Korea, +82-54-279-2348 (phone), +82-54-279-2199 (fax),

sukim@postech.ac.kr

Yoontae Lee, Room 388, POSTECH Biotech Center, 77 Cheongam-Ro, Nam-Gu, Pohang,

Gyeongbuk 37673, Republic of Korea, +82-54-279-2354 (phone), +82-54-279-0659 (fax),

yoontael@postech.ac.kr

List of abbreviations

HCC, Hepatocellular carcinoma; CIC, Capicua; TCGA, The cancer genome atlas; DEN,

Diethylnitrosamine; PEA3, Polyoma enhancer activator 3; ETV4, ETS translocation variant 4;

MMP, Matrix metalloproteinase; ERK, Extracellular signal–regulated kinase; RTK, Receptor

tyrosine kinase; shCIC, shRNA against *CIC*; *Cic* LKO, liver-specific *Cic* null mice

Abstract

Hepatocellular carcinoma (HCC) is developed by multiple steps accompanying progressive alterations of gene expression, which leads to increased cell proliferation and malignancy. Although environmental factors and intracellular signaling pathways that are critical for HCC progression have been identified, gene expression changes and the related genetic factors contributing to HCC pathogenesis are still insufficiently understood. In this study, we identify a transcriptional repressor Capicua/CIC as a suppressor of HCC progression and a potential therapeutic target. Expression of CIC is posttranscriptionally reduced in HCC cells. CIC levels are correlated with survival rates in patients with HCC. CIC overexpression suppresses HCC cell proliferation and invasion, whereas loss of CIC exerts opposite effects *in vivo* as well as *in vitro*. The levels of *PEA3* group genes, the best-known CIC target genes, are correlated with lethality in patients with HCC. Among the *PEA3* group genes, *ETV4* is the most significantly upregulated gene in CIC-deficient HCC cells, consequently promoting HCC progression. Furthermore, ETV4 induces expression of *MMP1*, the *MMP* gene highly relevant to HCC progression, in HCC cells, and knockdown of *MMP1* completely blocks the CIC deficiency-induced HCC cell proliferation and invasion. *Conclusion:* Our study demonstrates that the CIC-ETV4-MMP1 axis is a novel regulatory module controlling HCC progression.

4

Introduction

Hepatocellular carcinoma (HCC) is the second leading cause of cancer-related death worldwide and the fifth most common malignancy, especially in East Asia and South Africa (1, 2). In most cases, human HCC is driven by chronic hepatitis B virus (HBV) or hepatitis C virus (HCV) infections, alcoholic abuse, non-alcoholic fatty liver disease, autoimmune hepatitis, diabetes mellitus, and several metabolic diseases (3).

Among multiple therapeutic strategies to overcome HCC, liver resection is still the best therapeutic strategy to treat HCC with a 5-year survival rate in approximately 70% (3). Another option of HCC treatment is the orthotopic liver transplantation, which has the lowest risk of tumor recurrence but is applied to very few patients. Radiofrequency ablation (RFA) and trans-arterial chemoembolization (TACE) are other therapeutic strategies but have marginal effects. Because of these limitations of HCC treatment, many studies are focused on finding molecular therapies for HCC. Sorafenib, a related multikinase inhibitor, is currently the only drug approved for advanced HCC management. Despite sorafenib treatment, overall survival is increased by only 37%, with several major side effects including acne-like rash, diarrhea, fatigue, and hypertension (4).

In search for a better understanding and efficacious treatment in HCC, many cancer drivers and molecular therapies have been reported (5). Some studies have explored HCC genomic alterations and identified frequently mutated genes, including *TERT* promoter, *TP53*, and *CTNNB1* (β-catenin) (6, 7). In addition, chromosomal amplifications (1q, 6p, 8q, 11q, 17q, and 20q) and deletions (4q, 8p, 13q, 16q, and 17p) that affect important oncogenes and tumor suppressors have been identified in samples from patients with HCC (8). Moreover, several

signaling pathways are investigated to be targeted by novel therapies for HCC including RAS, TGF-β, FGF-19/FGFR-4, and MET signaling pathways (9). Importantly, RAS signaling is related to cell survival and proliferation and is activated in more than 50% of HCCs (10, 11) . Although HCC progression is considered as a multistep and a long-term progressive process, the precise molecular mechanism of HCC pathogenesis remains largely unknown (12).

Capicua/CIC is a transcriptional repressor that is highly conserved from *C. elegans* to humans (13). There are two main isoforms of CIC, the short (CIC-S) and long (CIC-L) form, which differ in their amino-terminal portions. CIC has two highly conserved domains: a DNA-binding high mobility group (HMG) box domain and a carboxy-terminal motif (C1) (13). CIC preferentially recognizes T(G/C)AATG(G/A)A sequences through the HMG-box and C1 domains to repress expression of its target genes in *Drosophila* and mammals (14-16). CIC activity can be regulated by receptor tyrosine kinase (RTK) signaling pathways in *Drosophila* and mammals (17-19). Activation of RTK-MAPK pathways phosphorylates CIC, resulting in degradation and/or cytoplasmic localization of CIC (20, 21).

Cic was firstly identified in a screen for mutations affecting tissue patterning in *Drosophila* embryo (17). In *Drosophila*, several studies revealed that Cic regulates not only anteroposterior and dorsoventral body patterning, but also intestinal stem cell proliferation (22), wing development (23), and other processes in development (24).

In mammals, CIC has been implicated in pathogenesis of spinocerebellar ataxia type-1 neurodegenerative disease (25), as well as regulation of essential processes such as lung alveolarization (26), liver homeostasis (27), learning and memory (28), and follicular helper T cell differentiation (29). CIC has also been studied in several cancer contexts, and its mutations were found in soft tissue, brain, lung, gastric, prostate, and breast cancers (14, 21, 30-32).

6

Furthermore, CIC directly suppresses expression of *PEA3* group genes (*ETV1*, *ETV4*, and *ETV5*), which are known to be frequently overexpressed in many cancers and have tumor-promoting functions (14, 30, 33, 34).

Although increasing evidences have indicated that CIC functions as a tumor suppressor in various cancers (19, 21, 35, 36), no studies have examined its clinicopathologic significance and molecular functions in HCC. In this study, we present the first evidence that decreased level of CIC is associated with HCC progression and indicates poor prognosis. Both *in vitro* and *in vivo* assays demonstrate that CIC has a tumor suppressive function in the progression of HCC. Molecular studies reveal that CIC regulates *ETV4* expression in HCC cells and that MMP1 acts as a key downstream target of the CIC-ETV4 axis in HCC context. Therefore, our findings suggest that CIC-ETV4-MMP1 regulatory axis might have a critical role in HCC progression.

Experimental procedures

Tissue microarray and immunohistochemistry

Two liver cancer tissue microarrays with liver tumors and adjacent normal liver tissues (LV1221 and LV6161) were purchased from Biomax (MD, USA). Formalin-fixed paraffin-embedded specimens were de-paraffinized and stained with rabbit polycolonal anti-CIC antibody. Each sample stained with anti-CIC antibody was scored as negative (-), weak (+), moderate (++), or strong (+++) according to the staining intensity. These scores were determined independently by two pathologists. The scoring by the pathologists was done in a blinded manner.

Induction of HCC in mice

To induce HCC, diethylnitrosamine (DEN, Sigma-Aldrich, MO, USA) was injected intraperitoneally (i.p.) into 2-week-old male mice (5 μg/g). For tumor formation analysis, mice were sacrificed to prepare liver tissues at 8 months after DEN treatment. Externally visible tumors (>1 mm) on liver were counted and measured. Livers were micro-dissected into tumor and non-tumor and stored at −80°C until analyzed by qRT-PCR.

Lung metastasis and survival were analyzed at 15 months after DEN treatment. The survival of the mice was recorded weekly. After 15 months, the mice were sacrificed, and their lungs were dissected, paraffin-embedded, and used for H&E staining. Serial sections of entire lung tissues were conducted. Four sections per each lung tissue were chosen for H&E staining. Total number of metastasized tumor lesions was counted from the H&E-stained sections and used for calculation of the average number of tumor foci in a lung tissue per each genotype.

8

Other assays used in this study are described in the Supporting Information.

Results

Inverse correlation between CIC protein levels and HCC severity

Since the role of CIC in HCC development and progression has not yet been determined, we analyzed The Cancer Genome Atlas (TCGA) data sets for patients with HCC (Table S1) in order to gain insight on the relevance between CIC and HCC pathogenesis. *CIC* mRNA levels were not downregulated, but rather increased in HCC tissue samples compared with normal liver tissues (Fig. 1A). However, the survival rate was significantly decreased in HCC patients with low levels of *CIC* (the lower 20%, n=74) compared with those with high levels of *CIC* (the upper 20%, n=74) (Fig. 1B and Table S2). Previous studies have demonstrated that activation of EGFR and its downstream signaling molecules, which promotes tumorigenesis and cancer metastasis, inactivates CIC via either degradation or cytoplasmic translocation (20, 21). Moreover, we have shown that CIC protein levels were dramatically decreased in prostatic adenocarcinoma (35). Thus, we examined CIC protein levels in normal liver and HCC tissues on tissue microarrays by immunohistochemistry using anti-CIC antibody. Reduced expression of CIC was more frequently observed in HCC samples than in normal liver tissues (Fig. 1C). To directly address whether CIC expression decreases in HCC tissues at protein level, but not at mRNA level, we examined expression profiles of both CIC protein and *CIC* mRNA in the same tissue samples of normal liver and HCC of different pathological stages (Table S3). Most HCC tissues showed reduction in CIC protein levels compared with normal liver tissues, whereas *CIC* mRNA level was not correlated with CIC protein level in each tissue sample (Fig. 1D), suggesting the posttranscriptional regulation of CIC expression in HCC cells. Taken together, these data indicate the association of CIC levels with HCC progression.

10

CIC suppresses HCC progression

To test whether CIC has a suppressive function in HCC progression, we examined the effect of CIC overexpression on HCC cell growth and invasion. We chose SK-HEP-1 and MHCC-97H cells, which are highly metastatic and aggressive HCC cell lines (37, 38), for the experiments, because they express relatively low levels of CIC compared with other HCC cell lines (Fig. S1). Forced expression of either CIC-S or CIC-L suppressed cell proliferation, invasion, and migration in both cell lines (Figs. 2A-D). Then, we tested whether suppression of CIC expression has the opposite effects. HCC cells that stably express shRNA against *CIC* (shCIC) had increased proliferation rate and invasive and migratory activity compared with control HCC cells (Figs. 2E-H). CRISPR-Cas9-mediated knockout of *CIC* also promoted HCC cell proliferation and invasion (Fig. S2). We confirmed these results *in vivo* using xenograft mouse models. Control and shCIC-expressing SK-HEP-1 or MHCC-97H cells were subcutaneously injected into either posterior flank of the same nude mice, respectively, and tumor volume was measured every week. The CIC-deficient HCC cells grew more rapidly and formed larger tumor mass than the control cells (Fig. 3A). To compare metastatic activity between control and CIC-deficient HCC cells, the cells were intravenously injected into nude mice followed by quantification of GFP signal, which is expressed from shRNA-expressing lentiviral vectors (pGIPZ), in lung tissues. The CIC-deficient HCC cells had higher degree and frequency of metastasis to lung than control cells (Figs. 3B, C). Taken together, these findings indicate that CIC functions as a negative regulator in HCC progression.

Increased lung metastasis and lethality in *Cic*-deficient mice treated with DEN

To better understand *in vivo* effect of CIC deficiency on HCC progression, we generated mice

with a specific deletion of *Cic* alleles in hepatocytes (*Cic^{f/f};Alb-Cre*, *Cic* LKO) (Fig. 4A) and

induced liver cancer in these mice by treatment with diethylnitrosamine (DEN). WT (*Cic^{f/f}*) and

Cic LKO mice were intraperitoneally injected with DEN at 2 weeks of age and subjected to

analyses of tumorigenesis, lung metastasis, and viability (Fig. 4B). Tumor formation on liver

tissues was comparable between WT and *Cic* LKO mice at 8 months of age (Fig. 4C). However,

lung metastasis was substantially increased in *Cic* LKO mice at 15 months of age (Fig. 4D).

Moreover, about 30% of *Cic* LKO mice died after 1 year of age, whereas none of WT mice did

(Fig. 4E). These results demonstrate that reduction in CIC expression can critically contribute to

promotion of HCC progression, which is consistent with the finding that the survival rate was

decreased in the HCC patients with low levels of *CIC* (Fig. 1B).

ETV4 is a critical CIC target that promotes HCC progression

Many studies have shown that *PEA3* group genes, which include *ETV1*, *ETV4*, and *ETV5*, are

direct target genes of CIC (14, 19, 25, 26) and that overexpression of these genes promotes

proliferation and invasion of various types of cancer cell (33). However, the role of PEA3 group

transcription factors in HCC progression has not yet been comprehensively understood.

Therefore, we analyzed expression profiles of *PEA3* group genes and association of these gene

expression levels with lethality in patients with HCC using the TCGA database (Tables S1 and

S4). Among three genes, only *ETV4* levels were increased in all stages of HCC cells with

statistical significance compared with normal liver cells (Fig. 5A). On the other hand, overall

survival rates of HCC patients were inversely correlated with the levels of all *PEA3* group genes

12

(Fig. 5B), suggesting that PEA3 group transcription factors might also function as a tumor promoter in the context of HCC progression.

Next, we examined whether CIC regulates expression of *PEA3* group genes in HCC cells. The levels of *PEA3* group genes in control and shCIC-expressing HCC cells were determined by qRT-PCR analysis (Fig. 5C). Among three genes, *ETV4* levels were most significantly upregulated in three different HCC cell lines with *CIC* RNAi (Fig. 5C). Knockdown of *CIC* did not increase levels of *PEA3* group genes in HepG2 cells (Fig. 5C), suggesting that CIC differentially regulates its target gene expression in a cell-type dependent manner, which is consistent with previous findings (27, 35, 39). Furthermore, the upregulation of ETV4 expression in *CIC* knockdown HCC cells was confirmed at protein level (Fig. 5D). Increases in *Etv4* levels were also most apparent in both normal liver and DEN-induced tumor tissues from *Cic* LKO mice compared with those in *Etv1* and *Etv5* (Figs. 5E-G). Overall, these data suggest that, among *PEA3* group genes, *ETV4* is a major target gene of CIC in hepatic cells.

Given that *ETV4* had the highest relevance to HCC progression (Figs. 5A, B) and that *ETV4* expression was most significantly regulated by CIC in HCC cells (Fig. 5C), we focused on the role of ETV4 in HCC progression. We first tested whether ETV4 has HCC-promoting activity. Overexpression of ETV4 indeed increased cell proliferation, invasion, and migration in HCC cells (Figs. 6A-D and S3). We next examined whether the increased cell proliferation, invasion, and migration in CIC-deficient HCC cells were due to derepression of *ETV4*. Knockdown of *ETV4* completely blocked the CIC deficiency-mediated promotion of HCC progression (Fig. 6E-H), demonstrating that *ETV4* is a key target gene of CIC in regulation of HCC progression.

Regulation of *MMP1* expression by the CIC-ETV4 axis in HCC cells

Matrix metalloproteinases (MMPs) promote cancer progression through various ways including destruction of extracellular matrix, activation of growth factors, suppression of apoptosis, and induction of angiogenesis (40). Therefore, MMPs are the principle mediators of cancer progression and frequently used as biomarkers for various types of cancer. There are 23 members of MMP in humans. Previous studies revealed that PEA3 group transcription factors activate expression of various *MMP* genes and that most *MMP* genes harbor ETS binding elements in their promoters (26, 41). To gain insight on which MMPs are critically involved in HCC progression, we analyzed the relevance of each *MMP* to HCC progression using the TCGA database (Tables S1 and S5), as we did for *CIC* and *PEA3* group genes. Among 23 *MMP* genes, levels of *MMP1*, *MMP9*, *MMP10*, *MMP11*, *MMP12*, and *MMP14* were significantly higher in HCC tissues than in normal liver tissues (Figs. 7A and S4). Analysis of survival rates revealed that levels of *MMP1*, *MMP7*, *MMP10*, *MMP12*, *MMP16*, and *MMP26* were inversely correlated with survival rates of HCC patients with statistical significance (Figs. 7B and S5). Thus, these analyses identified *MMP1*, *MMP10*, and *MMP12* as *MMP* genes strongly associated with promotion of HCC progression.

Next, we investigated which of the selected *MMP* genes are regulated by the CIC-ETV4 axis in HCC cells. Among *MMP1*, *MMP10*, and *MMP12*, only *MMP1* expression was significantly induced by ETV4 overexpression in both SK-HEP-1 and MHCC-97H HCC cell lines (Fig. 7C). We confirmed that ETV4 enhances *MMP1* promoter activity by luciferase assay using *MMP1* promoter-containing reporter construct (Fig. 7D). We further examined regulation of *MMP1* expression by CIC in HCC cells. Knockdown of *CIC* significantly upregulated levels of *MMP1*, but neither *MMP10* nor *MMP12*, in SK-HEP-1 and MHCC-97H HCC cell lines (Fig. 7E). Consistent with this result, overexpression of CIC downregulated *MMP1* expression (Fig. S6).

14

On the other hand, expression of *MMP13*, which belongs to the interstitial collagenase family as MMP1 does and shares high amino acid identity (86%) with MMP1 (42), was not significantly affected by either ETV4 overexpression or *CIC* RNAi in HCC cells (Fig. S7), suggesting that the CIC-ETV4 axis might selectively regulate expression of *MMP1* rather than all members of the MMP subfamily with similar biochemical and pathological properties. The levels of *Mmp1a*, a mouse homolog of human *MMP1*, were also upregulated in liver tumors from 15-month-old *Cic* LKO mice treated with DEN compared with those from WT controls, while the levels of other *Mmp* genes including *Mmp2*, *Mmp9*, and *Mmp12*, which have been implicated in the promotion of HCC progression (43, 44), were comparable (Fig. S8). Overall, these results suggest that MMP1 might be a key effector MMP protein that functions at the downstream of the CIC-ETV4 axis in the context of HCC progression.

To directly address whether the increased expression of *MMP1* in CIC-deficient HCC cells was due to derepression of *ETV4*, we examined levels of *MMP1* in control and shCIC-expressing HCC cells treated with either control siRNA or siRNA against *ETV4*. Knockdown of *ETV4* certainly restored *MMP1* expression to the normal level in CIC-deficient HCC cells (Fig. 7F). Taken together, these data suggest that *MMP1* expression can be regulated by the CIC-ETV4 axis in the process of HCC progression.

CIC deficiency promotes HCC progression via *MMP1* overexpression
Since we identified *MMP1* as a critical downstream target gene of the CIC-ETV4 axis in HCC cells, we finally determined whether the induction of *MMP1* expression contributed to the enhanced cancer progression in CIC-deficient HCC cells. We transfected control and shCIC-expressing HCC cells with either control siRNA or two different siRNAs against *MMP1* and

examined cell proliferation, invasion, and migration. Knockdown of *MMP1* completely

suppressed the increased cell proliferation and invasive and migratory activity in shCIC-

expressing HCC cells (Figs. 8A-D), demonstrating that the increased expression of *MMP1*

indeed critically contributed to the CIC deficiency-mediated promotion of HCC progression.

16

Discussion

  In this study, we demonstrated for the first time that CIC could function as a negative regulator of HCC progression via control of ETV4-MMP1 axis (Fig. 8E). Overexpression of CIC suppressed HCC cell proliferation and invasion, whereas CIC deficiency promoted HCC progression *in vivo* as well as *in vitro*. We found a discrepancy between CIC-deficient HCC cells and DEN-induced HCC in liver-specific *Cic* null mice; CIC-deficient HCC cells had increased proliferation and invasive activity, while DEN-treated *Cic*-deficient mice exhibited the enhanced lung metastasis, but not tumor formation in livers. This finding implies that loss of CIC might not be enough to facilitate the onset of HCC, but nevertheless could contribute to the promotion of HCC progression once HCC has occurred.

  Analyses of the TCGA database and tissue samples from patients with HCC revealed that CIC expression is reduced in HCC cells at protein level, but not at mRNA level. These results suggest that HCC-promoting factors and/or signaling pathways might downregulate CIC expression in HCC cells at posttranscriptional level. It is well known that activation of RTK signaling suppresses CIC activity via degradation or cytoplasmic translocation of CIC in *Drosophila* and mammals (13, 20, 21, 25). In this process, ERK, a downstream effector kinase of RTK signaling pathways, plays a pivotal role. ERK can interact with CIC (45) and the inhibition of ERK rescues CIC activity in the context of EGFR activation (21). These findings suggest that activation of ERK and its upstream signaling cascades might be involved in downregulation of CIC protein levels. Many studies have demonstrated that RAS/RAF/MEK/ERK signaling pathway is associated with HCC pathogenesis (46, 47). Levels of total or phosphorylated ERK are often higher in HCC cells than in normal liver cells (48, 49). Moreover, it was reported that ERK is

mainly found in the nucleus of HCC cells (46). Therefore, it would be conceivable that the

decrease in CIC levels in HCC cells was due to the enhanced ERK activity (Fig. 8E).

Our study demonstrated the significant relevance of MMP1 to HCC progression. In the context

of HCC, functional significance of other MMPs, such as MMP2, MMP9, and MMP12, have

been more appreciated than that of MMP1 (43, 44). However, our comprehensive analyses for

MMP genes in HCC patients using the TCGA datasets indicated that MMP1 is more significantly

associated with HCC pathogenesis than other MMPs previously recognized to promote HCC

progression. The *in vitro* experiments using HCC cell lines showed that MMP1 deficiency is

sufficient to suppress HCC cell growth and invasion, underlying the critical role of MMP1 in

HCC progression. We also provided several evidences that MMP1 is a critical downstream target

of the CIC-ETV4 axis that contributes to the CIC deficiency-mediated promotion of HCC

progression. *MMP1* expression is under the control of ETV4 and knockdown of *MMP1*

completely blocks the increased cell proliferation and invasion in CIC-deficient HCC cells.

Nevertheless, it cannot be ruled out that other MMPs could also contribute to the enhanced cell

proliferation and invasion in CIC-deficient HCC cells, because most *MMP* genes have ETS

binding elements in their promoters (26). To better understand the molecular mechanism

underlying the CIC deficiency-mediated promotion of HCC progression, genome-wide

identification of target genes of CIC as well as ETV4 and studies on their roles in HCC

pathogenesis need to be followed.

This study suggests CIC-ETV4-MMP1axis as a novel genetic module that controls HCC

progression. Patients with HCC have a poor survival rate mainly due to late diagnosis (50).

Therefore, it is very important to identify genetic alterations that can predict HCC development

and progression as early as possible. In this regard, our findings provide novel candidate

18

molecules that might be potentially developed as diagnostic markers as well as therapeutic

targets for HCC.

References

1.   Shariff MI, Cox IJ, Gomaa AI, Khan SA, Gedroyc W, Taylor-Robinson SD. Hepatocellular carcinoma: current trends in worldwide epidemiology, risk factors, diagnosis and therapeutics. Expert Rev Gastroenterol Hepatol 2009;3:353-367.

2.   Jemal A, Bray F, Center MM, Ferlay J, Ward E, Forman D. Global cancer statistics. CA Cancer J Clin 2011;61:69-90.

3.   El-Serag HB. Hepatocellular Carcinoma. N Engl J Med 2011;365:1118-1127.

4.   Llovet JM, Ricci S, Mazzaferro V, Hilgard P, Gane E, Blanc J-F, de Oliveira AC, et al. Sorafenib in advanced hepatocellular carcinoma. N Engl J Med 2008;359:378-390.

5.   Llovet JM, Villanueva A, Lachenmayer A, Finn RS. Advances in targeted therapies for hepatocellular carcinoma in the genomic era. Nat Rev Clin Oncol 2015;12:408-424.

6.   **Totoki Y**, **Tatsuno K**, **Covington KR**, Ueda H, Creighton CJ, Kato M, Tsuji S, et al. Trans-ancestry mutational landscape of hepatocellular carcinoma genomes. Nat Genet 2014;46:1267-1273.

7.   **Schulze K**, **Imbeaud S**, **Letouzé E**, Alexandrov LB, Calderaro J, Rebouissou S, Couchy G, et al. Exome sequencing of hepatocellular carcinomas identifies new mutational signatures and potential therapeutic targets. Nat Genet 2015;47:505-511.

8.   Farazi PA, DePinho RA. Hepatocellular carcinoma pathogenesis: from genes to environment. Nat Rev Cancer 2006;6:674-687.

9.   Torrecilla S, Llovet JM. New molecular therapies for hepatocellular carcinoma. Clin Res Hepatol Gastroenterol 2015;39:S80-S85.

20

10.   Villanueva A, Newell P, Chiang DY, Friedman SL, Llovet JM. Genomics and signaling pathways in hepatocellular carcinoma. Semin Liv Dis 2007;27:55-76.

11.   Forner A, Llovet JM, Bruix J. Hepatocellular carcinoma. Lancet 2012;379:1245-1255.

12.   Zucman-Rossi J, Villanueva A, Nault JC, Llovet JM. Genetic Landscape and Biomarkers of Hepatocellular Carcinoma. Gastroenterology 2015;149:1226-1239.

13.   Jiménez G, Shvartsman SY, Paroush Ze. The Capicua repressor–a general sensor of RTK signaling in development and disease. J Cell Sci 2012;125:1383-1391.

14.   **Kawamura-Saito M**, **Yamazaki Y**, Kaneko K, Kawaguchi N, Kanda H, Mukai H, Gotoh T, et al. Fusion between CIC and DUX4 up-regulates PEA3 family genes in Ewing-like sarcomas with t (4; 19)(q35; q13) translocation. Hum Mol Genet 2006;15:2125-2137.

15.   **Ajuria L**, **Nieva C**, **Winkler C**, Kuo D, Samper N, Andreu MJ, Helman A, et al. Capicua DNA-binding sites are general response elements for RTK signaling in Drosophila. Development 2011;138:915-924.

16.   Forés M, Simón-Carrasco L, Ajuria L, Samper N, González-Crespo S, Drosten M, Barbacid M, et al. A new mode of DNA binding distinguishes Capicua from other HMG-box factors and explains its mutation patterns in cancer. PLoS Genet 2017;13:e1006622.

17.   Jiménez G, Guichet A, Ephrussi A, Casanova J. Relief of gene repression by torso RTK signaling: role of capicua in Drosophila terminal and dorsoventral patterning. Genes Dev 2000;14:224-231.

18.   Tseng A-SK, Tapon N, Kanda H, Cigizoglu S, Edelmann L, Pellock B, White K, et al. Capicua regulates cell proliferation downstream of the receptor tyrosine kinase/ras signaling pathway. Curr Biol 2007;17:728-733.

19.   Dissanayake K, Toth R, Blakey J, Olsson O, Campbell DG, Prescott AR, MacKintosh C. ERK/p90RSK/14-3-3 signalling has an impact on expression of PEA3 Ets transcription factors via the transcriptional repressor capicua. Biochem J 2011;433:515-525.

20.   **Grimm O**, **Sanchez Zini V**, Kim Y, Casanova J, Shvartsman SY, Wieschaus E. Torso RTK controls Capicua degradation by changing its subcellular localization. Development 2012;139:3962-3968.

21.   Okimoto RA, Breitenbuecher F, Olivas VR, Wu W, Gini B, Hofree M, Asthana S, et al. Inactivation of Capicua drives cancer metastasis. Nat Genet 2017;49:87-96.

22.   Jin Y, Ha N, Forés M, Xiang J, Gläßer C, Maldera J, Jiménez G, et al. EGFR/Ras signaling controls Drosophila intestinal stem cell proliferation via Capicua-regulated genes. PLoS Genet 2015;11:e1005634.

23.   Roch F, Jiménez G, Casanova J. EGFR signalling inhibits Capicua-dependent repression during specification of Drosophila wing veins. Development 2002;129:993-1002.

24.   Yang L, Paul S, Trieu KG, Dent LG, Froldi F, Forés M, Webster K, et al. Minibrain and Wings apart control organ growth and tissue patterning through down-regulation of Capicua. Proc Natl Acad Sci U S A 2016:10583-10588.

25.   Fryer JD, Yu P, Kang H, Mandel-Brehm C, Carter AN, Crespo-Barreto J, Gao Y, et al. Exercise and genetic rescue of SCA1 via the transcriptional repressor Capicua. Science 2011;334:690-693.

26.   Lee Y, Fryer JD, Kang H, Crespo-Barreto J, Bowman AB, Gao Y, Kahle JJ, et al. ATXN1 protein family and CIC regulate extracellular matrix remodeling and lung alveolarization. Dev Cell 2011;21:746-757.

27. Kim E, Park S, Choi N, Lee J, Yoe J, Kim S, Jung H-Y, et al. Deficiency of Capicua disrupts bile acid homeostasis. Sci Rep 2015;5:8272.

28. **Lu H-C**, **Tan Q**, Rousseaux MW, Wang W, Kim J-Y, Richman R, Wan Y-W, et al. Disruption of the ATXN1-CIC complex causes a spectrum of neurobehavioral phenotypes in mice and humans. Nat Genet 2017;49:527-536.

29. **Park S**, **Lee S**, **Lee C-G**, Park GY, Hong H, Lee J-S, Kim YM, et al. Capicua deficiency induces autoimmunity and promotes follicular helper T cell differentiation via derepression of ETV5. Nat Commun 2017;8:ncomms16037.

30. **Bettegowda C**, **Agrawal N**, Jiao Y, Sausen M, Wood LD, Hruban RH, Rodriguez FJ, et al. Mutations in CIC and FUBP1 contribute to human oligodendroglioma. Science 2011;333:1453-1455.

31. **Sjöblom T**, **Jones S**, **Wood LD**, **Parsons DW**, Lin J, Barber TD, Mandelker D, et al. The consensus coding sequences of human breast and colorectal cancers. Science 2006;314:268-274.

32. Kan Z, Jaiswal BS, Stinson J, Janakiraman V, Bhatt D, Stern HM, Yue P, et al. Diverse somatic mutation patterns and pathway alterations in human cancers. Nature 2010;466:869-873.

33. Oh S, Shin S, Janknecht R. ETV1, 4 and 5: an oncogenic subfamily of ETS transcription factors. Biochim Biophys Acta 2012;1826:1-12.

34. Sizemore GM, Pitarresi JR, Balakrishnan S, Ostrowski MC. The ETS family of oncogenic transcription factors in solid tumours. Nat Rev Cancer 2017;17:337-351.

35. Choi N, Park J, Lee J-S, Yoe J, Park GY, Kim E, Jeon H, et al. miR-93/miR-106b/miR-375-CIC-CRABP1: a novel regulatory axis in prostate cancer progression. Oncotarget 2015;6:23533-23547.

36.   Gleize V, Alentorn A, Connen de Kérillis L, Labussière M, Nadaradjane AA, Mundwiller E, Ottolenghi C, et al. CIC inactivating mutations identify aggressive subset of 1p19q codeleted gliomas. Ann Neurol 2015;78:355-374.

37.   **Ao J**, **Meng J**, **Zhu L**, Nie H, Yang C, Li J, Gu J, et al. Activation of androgen receptor induces ID1 and promotes hepatocellular carcinoma cell migration and invasion. Mol Oncol 2012;6:507-515.

38.   Hao Q, Li T, Zhang X, Gao P, Qiao P, Li S, Geng Z. Expression and roles of fatty acid synthase in hepatocellular carcinoma. Oncol Rep 2014;32:2471-2476.

39.   LeBlanc VG, Firme M, Song J, Chan SY, Lee MH, Yip S, Chittaranjan S, et al. Comparative transcriptome analysis of isogenic cell line models and primary cancers links capicua (CIC) loss to activation of the MAPK signalling cascade. J Pathol 2017;242:206-220.

40.   Egeblad M, Werb Z. New functions for the matrix metalloproteinases in cancer progression. Nat Rev Cancer 2002;2:161-174.

41.   Ye S. Polymorphism in matrix metalloproteinase gene promoters: implication in regulation of gene expression and susceptibility of various diseases. Matrix Biol 2000;19:623-629.

42.   Foley CJ, Kuliopulos A. Mouse matrix metalloprotease-1a (Mmp1a) gives new insight into MMP function. J Cell Physiol 2014;229:1875-1880.

43.   Ng KT-P, Qi X, Kong K-L, Cheung BY-Y, Lo C-M, Poon RT-P, Fan S-T, et al. Overexpression of matrix metalloproteinase-12 (MMP-12) correlates with poor prognosis of hepatocellular carcinoma. Eur J Cancer 2011;47:2299-2305.

44.   Määttä M, Soini Y, Liakka A, Autio-Harmainen H. Differential expression of matrix metalloproteinase (MMP)-2, MMP-9, and membrane type 1-MMP in hepatocellular and

24

pancreatic adenocarcinoma: implications for tumor progression and clinical prognosis. Clin Cancer Res 2000;6:2726-2734.

45.   Futran AS, Kyin S, Shvartsman SY, Link AJ. Mapping the binding interface of ERK and transcriptional repressor Capicua using photocrosslinking. Proc Natl Acad Sci U S A 2015;112:8590-8595.

46.   Li L, Zhao GD, Shi Z, Qi LL, Zhou LY, Fu ZX. The Ras/Raf/MEK/ERK signaling pathway and its role in the occurrence and development of HCC. Oncol Lett 2016;12:3045-3050.

47.   Yang S, Liu G. Targeting the Ras/Raf/MEK/ERK pathway in hepatocellular carcinoma. Oncol Lett 2017;13:1041-1047.

48.   Ito Y, Sasaki Y, Horimoto M, Wada S, Tanaka Y, Kasahara A, Ueki T, et al. Activation of mitogen‑activated protein kinases/extracellular signal‑regulated kinases in human hepatocellular carcinoma. Hepatology 1998;27:951-958.

49.   Yoshida T, Hisamoto T, Akiba J, Koga H, Nakamura K, Tokunaga Y, Hanada S, et al. Spreds, inhibitors of the Ras/ERK signal transduction, are dysregulated in human hepatocellular carcinoma and linked to the malignant phenotype of tumors. Oncogene 2006;25:6056-6066.

50.   Hernaez R, El‑Serag HB. Hepatocellular carcinoma surveillance: The road ahead. Hepatology 2017;65:771-773.

Author names in bold designate shared co-first authorship.

25

Acknowledgment

26

Figure legends

Figure 1. Decreased CIC protein levels in HCC cells and its correlation with poor survival rates in HCC patients. A. Analysis of TCGA database for expression levels of *CIC* mRNA in normal liver (NL) and HCC samples of four different clinicopathologic stages (I, II, III, and IV). The numbers in parentheses mean the number of subjects in each group. ***$P < 0.001$. **B**. Kaplan-Meier analysis of overall survival for HCC patients with high (the upper 20%) or low (the lower 20%) *CIC* expression (74 patients per each subgroup). *$P < 0.05$. **C**. Analysis of CIC protein levels in normal liver (n=33) and HCC (n=554) tissues using tissue microarrays. Immunohistochemical staining of CIC was conducted. Representative immunohistochemistry images showing four different expression levels of CIC in normal liver and HCC tissues were presented in the left panel. Scale bars indicate 100 μm. The right panel shows the proportion of tissue samples with different CIC expression scores. **D**. Western blot and qRT-PCR analyses of CIC expression profiles in normal liver (NL) and HCC samples.

Figure 2. CIC suppresses cell proliferation, migration, and invasion in HCC cells. A. Western blot analysis for ectopic expression of CIC-S and CIC-L in HCC cells (SK-HEP-1 and MHCC-97H). **B**. Cell growth assay of control and CIC-overexpressing HCC cells. **C**. Matrigel invasion assay of control and CIC-overexpressing HCC cells. The bottom panel is a bar graph for quantification of cell invasiveness. **D**. Transwell migration assay of control and CIC-overexpressing HCC cells. The bottom panel is a bar graph for quantification of cell migration. **E**. Western blot analysis showing knockdown efficiency of shCIC in HCC cells. shNC is for a negative control shRNA. **F**. Cell growth assay of control and shCIC-expressing HCC cells. **G**.

Matrigel invasion assay of control and shCIC-expressing HCC cells. The right panel is a bar

graph for quantification of cell invasiveness. **H**. Transwell migration assay of control and shCIC-

expressing HCC cells. The right panel is a bar graph for quantification of cell migration. Three

independent experiments were performed. All error bars show s.e.m. *$P < 0.05$, **$P < 0.01$, and

***$P < 0.001$.

Figure 3. CIC deficiency promotes tumor growth and metastasis *in vivo*. A. *In vivo*

subcutaneous tumor growth curves of SK-HEP-1 and MHCC-97H cells with shNC- or shCIC-

lentiviral infection. n=12 per each group. The middle panel is a representative image of xenograft

tumors dissected from the mice after the last measurement of tumor size. The right panel is a

graph for average weights of the dissected tumors. **B**. *In vivo* imaging of lung tissues into which

intravenously-injected control or shCIC-expressing SK-HEP-1 and MHCC-97H cells

metastasized. GFP signals expressed in the injected cells are shown as dot plots. The right panel

is a bar graph for quantification of GFP signals. n=10 per each group. All error bars show s.e.m.

*$P < 0.05$ and **$P < 0.01$. **C**. A bar graph for the incidence (black area) of lung metastasis in

each group of the nude mice.

Figure 4. Enhanced lung metastasis in liver-specific *Cic* null mice treated with DEN. A.

Western blot images of CIC and β-actin (loading control) in liver and lung tissues of wild-type

(WT) and liver-specific *Cic* null (*Cic* LKO) mice. **B.** Experimental scheme for analysis of

tumorigenesis and lung metastasis of HCC in mice treated with diethylnitrosamine (DEN). **C**.

Representative images of tumor-bearing livers from 8-month-old WT and *Cic* LKO mice treated

with DEN. Arrows indicate tumor foci. The right panel is a bar graph for the average numbers of

tumor foci on liver tissues of the DEN-treated WT and *Cic* LKO mice at 8 months of age. n=6

per each group. **D**. Representative images of H&E-stained lung tissues of DEN-treated WT and

Cic LKO mice at 15 months of age. The right panel is a bar graph for the average numbers of

tumor lesions in randomly selected lung tissue sections. Numbers of WT and *Cic* LKO mice used

for this analysis are 10 and 8, respectively. **E**. Kaplan–Meier survival curve of the DEN-treated

WT (n=11) and *Cic* LKO mice (n=11). All error bars show s.e.m. $*P < 0.05$.

Figure 5. ***ETV4 is a major CIC target with the most significant relevance to HCC among***

PEA3 group genes. **A**. Analysis of TCGA database for expression levels of *ETV1, ETV4*, and

ETV5 in normal liver (NL) and HCC samples of four different clinicopathologic stages (I, II, III,

and IV). The numbers in parentheses mean the number of subjects in each group. **B**. Kaplan-

Meier analysis of overall survival for HCC patients with high or low expression of *PEA3* group

genes (74 patients per each subgroup). **C**. qRT-PCR analysis of *PEA3* group gene expression

levels in control and *CIC* knockdown HCC cells. Experiments were performed more than three

times, independently. **D**. Western blot analysis for levels of ETV4 in control and *CIC*

knockdown HCC cells. **E**. qRT-PCR analysis for levels of *Cic, Etv1, Etv4*, and *Etv5* in livers of

7-week-old WT and *Cic* LKO mice. n=6 per each genotype. **F and G**. qRT-PCR analysis for

levels of *Cic*, *Etv1*, *Etv4*, and *Etv5* in liver tumors harvested from the DEN-treated WT and *Cic*

LKO mice at 8 months of age (**F**) and at 15 months of age (**G**). n=5 per each genotype. All error

bars show s.e.m. $*P < 0.05$, $**P < 0.01$, and $***P < 0.001$.

Figure 6. CIC deficiency-mediated promotion of HCC progression is due to derepression of

ETV4. **A**. Western blot analysis showing ectopic expression of ETV4 in SK-HEP-1 and MHCC-

97H cells. **B-D**. Cell growth assay (**B**), matrigel invasion assay (**C**), and transwell migration

assay (**D**) of control and ETV4-overexpressing HCC cells. **E**. qRT-PCR analysis for *ETV4*

mRNA levels in control and *CIC* knockdown HCC cells transfected with either control or *ETV4*

siRNA. NN: control HCC cells transfected with control siRNA, N4: control HCC cells

transfected with *ETV4* siRNA (siETV4), CN: *CIC* knockdown HCC cells transfected with

control siRNA, and C4: *CIC* knockdown HCC cells transfected with siETV4. **F-H**. Cell growth

assay (**F**), matrigel invasion assay (**G**), and transwell migration assay (**H**) of control and *CIC*

knockdown HCC cells treated with either control or *ETV4* siRNA. Three independent

experiments were performed. All error bars show s.e.m. *$P < 0.05$, **$P < 0.01$, and ***$P <$

0.001.

Figure 7. *MMP1 expression is regulated by the CIC-ETV4 axis.* **A**. Analysis of TCGA

database for expression levels of *MMP1* in normal liver (NL) and HCC samples of four different

clinicopathologic stages (I, II, III, and IV). The numbers in parentheses mean the number of

subjects in each group. **B**. Kaplan-Meier analysis of overall survival for HCC patients with high

or low *MMP1* expression (74 patients per each subgroup). **C**. qRT-PCR analysis for levels of

MMP1, *MMP10*, and *MMP12* in control and ETV4-overexpressing HCC cells (SK-HEP-1 and

MHCC-97H). **D**. Dual luciferase assay for regulation of *MMP1* promoter activity by ETV4. The

left panel is a schematic illustration for the luciferase reporter construct harboring *MMP1*

promoter region (-663/+1), in which there are two putative ETV4 binding sites (-323/-319 and -

155/-149). The right panel is a bar graph for relative luciferase activity in the presence or

absence of ETV4 overexpression. **E**. qRT-PCR analysis for levels of *MMP1*, *MMP10*, and

MMP12 in control and *CIC* knockdown HCC cells. **F**. qRT-PCR analysis for *MMP1* levels in

control and *CIC* knockdown HCC cells treated with either control or *ETV4* siRNA. NN: control HCC cells transfected with control siRNA, N4: control HCC cells transfected with siETV4, CN: *CIC* knockdown HCC cells transfected with control siRNA, and C4: *CIC* knockdown HCC cells transfected with siETV4. Three independent experiments were performed. All error bars show s.e.m. *$P < 0.05$, **$P < 0.01$, and ***$P < 0.001$.

Figure 8. Upregulation of *MMP1* expression contributes to the increased cell proliferation and invasion in *CIC* knockdown HCC cells. A. qRT-PCR analysis for *MMP1* levels in control and *CIC* knockdown HCC cells treated with either control or *MMP1* siRNAs. NN: control HCC cells transfected with control siRNA, N1-1: control HCC cells transfected with *MMP1* siRNA-1 (siMMP1-1), N1-2: control HCC cells transfected with *MMP1* siRNA-2 (siMMP1-2), CN: *CIC* knockdown HCC cells transfected with control siRNA, C1-1: *CIC* knockdown HCC cells transfected with siMMP1-1, and C1-2: *CIC* knockdown HCC cells transfected with siMMP1-2. **B-D**. Cell proliferation assay (**B**), matrigel invasion assay (**C**), and transwell migration assay (**D**) of control and *CIC* knockdown HCC cells treated with either control or *MMP1* siRNAs. Three independent experiments were performed. All error bars show s.e.m. *$P < 0.05$, **$P < 0.01$, and ***$P < 0.001$. **E**. Proposed model for the regulation of HCC progression by CIC-ETV4-MMP1 axis.
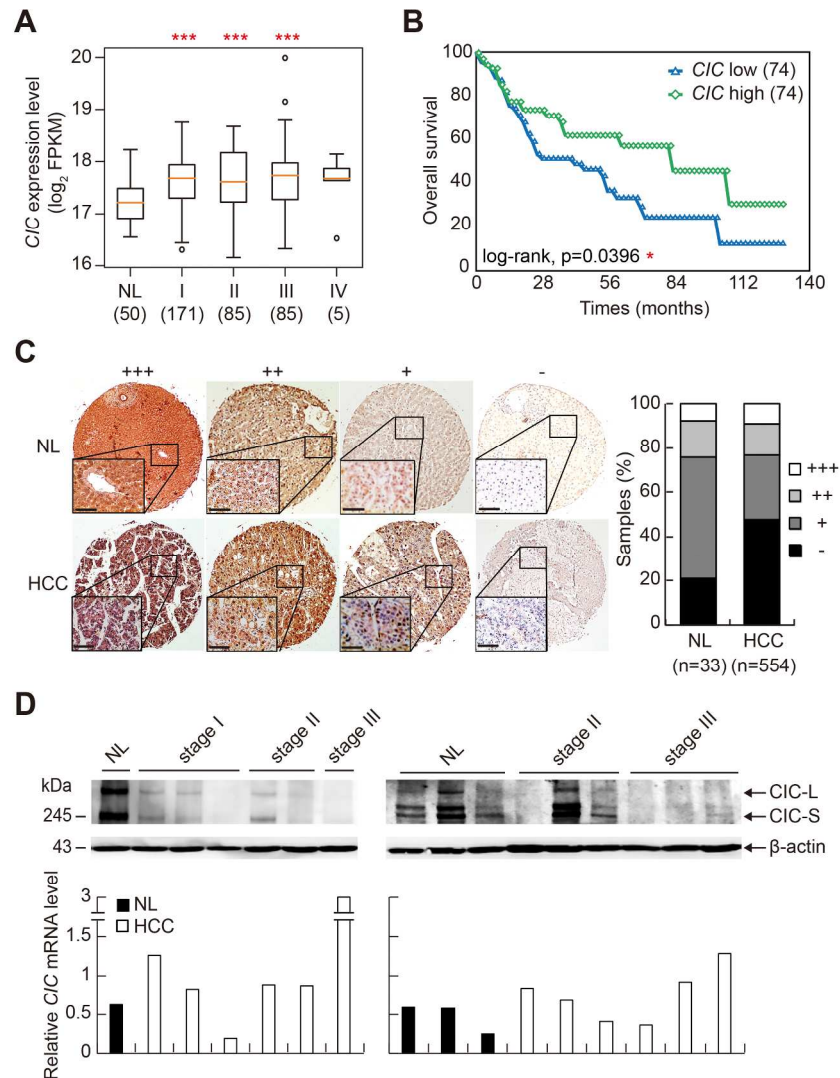
Fig. 1

Figure 1. Decreased CIC protein levels in HCC cells and its correlation with poor survival rates in HCC patients. A. Analysis of TCGA database for expression levels of CIC mRNA in normal liver (NL) and HCC samples of four different clinicopathologic stages (I, II, III, and IV). The numbers in parentheses mean the number of subjects in each group. ***$P < 0.001$. B. Kaplan-Meier analysis of overall survival for HCC patients with high (the upper 20%) or low (the lower 20%) CIC expression (74 patients per each subgroup). *$P < 0.05$. C. Analysis of CIC protein levels in normal liver (n=33) and HCC (n=554) tissues using tissue microarrays. Immunohistochemical staining of CIC was conducted. Representative immunohistochemistry images showing four different expression levels of CIC in normal liver and HCC tissues were presented in the left panel. Scale bars indicate 100 μm. The right panel shows the proportion of tissue samples with different CIC expression scores. D. Western blot and qRT-PCR analyses of CIC expression profiles in normal liver (NL) and HCC samples.
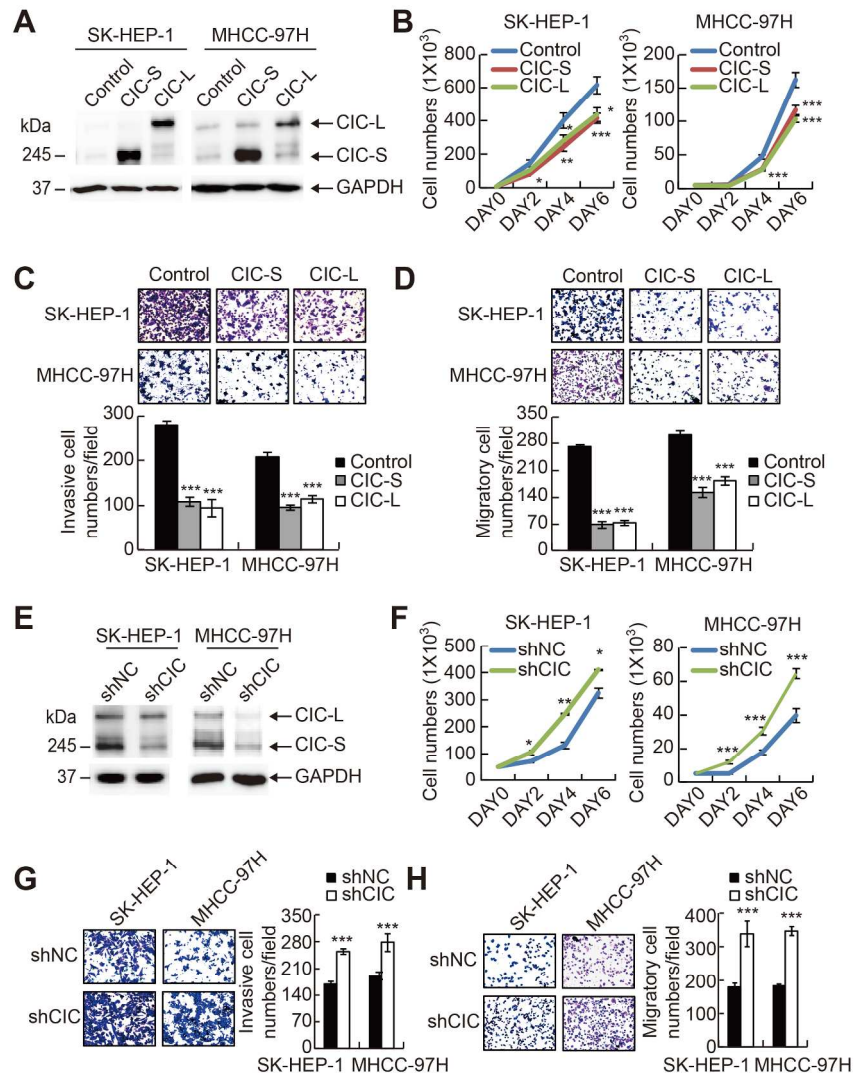
204x269mm (300 x 300 DPI)

Fig. 2

Figure 2. CIC suppresses cell proliferation, migration, and invasion in HCC cells. A. Western blot analysis for ectopic expression of CIC-S and CIC-L in HCC cells (SK-HEP-1 and MHCC-97H). B. Cell growth assay of control and CIC-overexpressing HCC cells. C. Matrigel invasion assay of control and CIC-overexpressing HCC cells. The bottom panel is a bar graph for quantification of cell invasiveness. D. Transwell migration assay of control and CIC-overexpressing HCC cells. The bottom panel is a bar graph for quantification of cell migration. E. Western blot analysis showing knockdown efficiency of shCIC in HCC cells. shNC is for a negative control shRNA. F. Cell growth assay of control and shCIC-expressing HCC cells. G. Matrigel invasion assay of control and shCIC-expressing HCC cells. The right panel is a bar graph for quantification of cell invasiveness. H. Transwell migration assay of control and shCIC-expressing HCC cells. The right panel is a bar graph for quantification of cell migration. Three independent experiments were performed. All error bars show s.e.m. *P < 0.05, **P < 0.01, and ***P < 0.001.
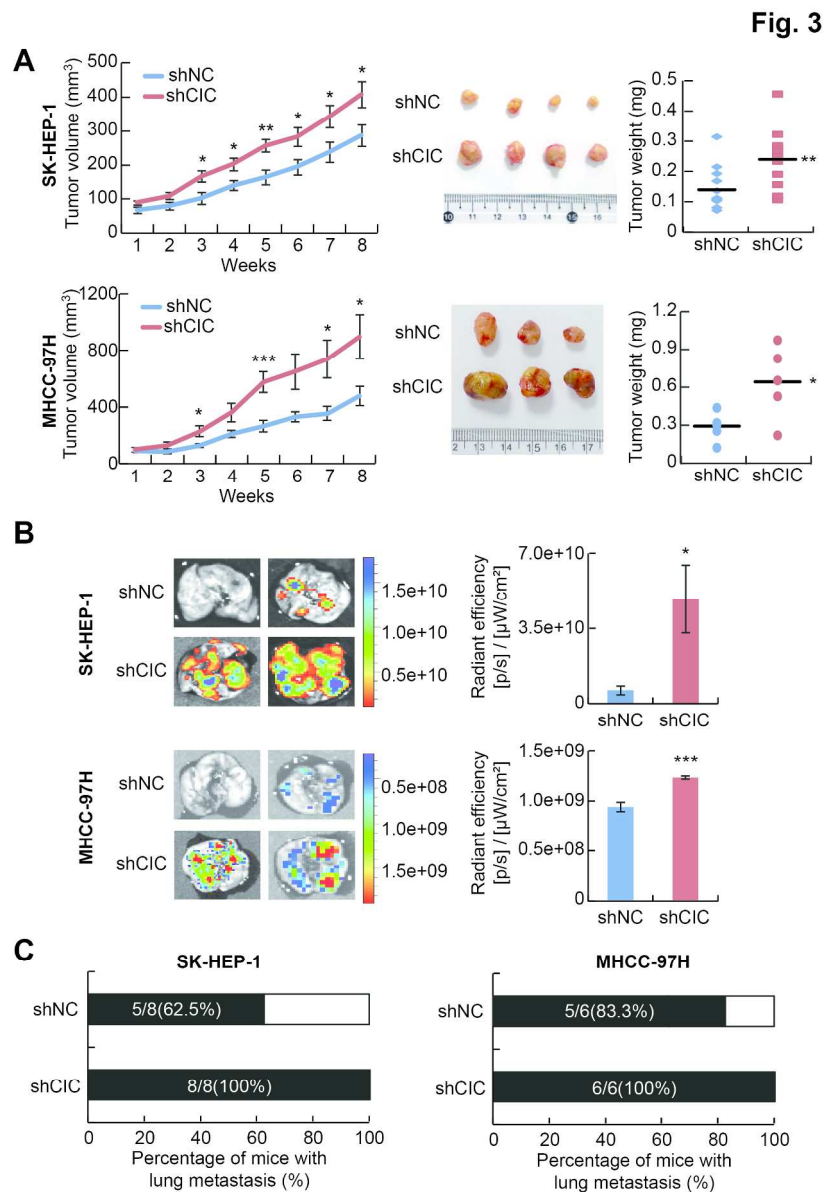
206x268mm (300 x 300 DPI)

Fig. 3

Figure 3. CIC deficiency promotes tumor growth and metastasis in vivo. A. In vivo subcutaneous tumor growth curves of SK-HEP-1 and MHCC-97H cells with shNC- or shCIC-lentiviral infection. n=12 per each group. The middle panel is a representative image of xenograft tumors dissected from the mice after the last measurement of tumor size. The right panel is a graph for average weights of the dissected tumors. B. In vivo imaging of lung tissues into which intravenously-injected control or shCIC-expressing SK-HEP-1 and MHCC-97H cells metastasized. GFP signals expressed in the injected cells are shown as dot plots. The right panel is a bar graph for quantification of GFP signals. n=10 per each group. All error bars show s.e.m. *P < 0.05 and **P < 0.01. C. A bar graph for the incidence (black area) of lung metastasis in each group of the nude mice.
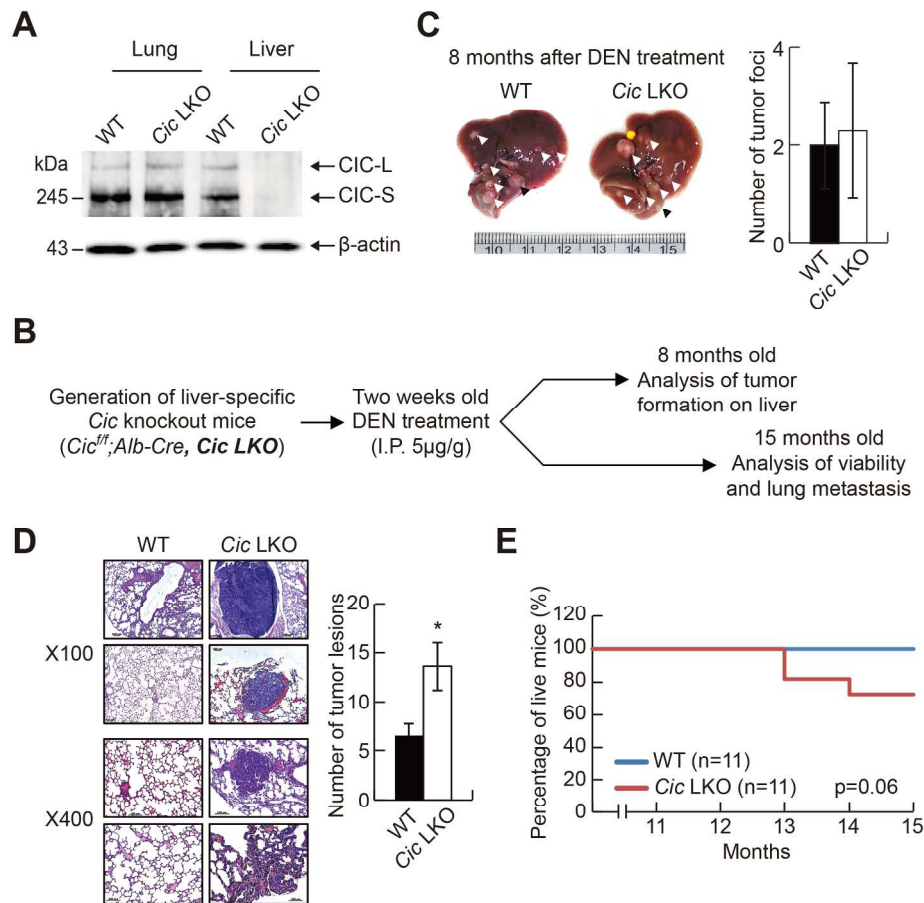
205x277mm (300 x 300 DPI)

Fig. 4

Figure 4. Enhanced lung metastasis in liver-specific Cic null mice treated with DEN. A. Western blot images of CIC and β-actin (loading control) in liver and lung tissues of wild-type (WT) and liver-specific Cic null (Cic LKO) mice. B. Experimental scheme for analysis of tumorigenesis and lung metastasis of HCC in mice treated with diethylnitrosamine (DEN). C. Representative images of tumor-bearing livers from 8-month-old WT and Cic LKO mice treated with DEN. Arrows indicate tumor foci. The right panel is a bar graph for the average numbers of tumor foci on liver tissues of the DEN-treated WT and Cic LKO mice at 8 months of age. n=6 per each group. D. Representative images of H&E-stained lung tissues of DEN-treated WT and Cic LKO mice at 15 months of age. The right panel is a bar graph for the average numbers of tumor lesions in randomly selected lung tissue sections. Numbers of WT and Cic LKO mice used for this analysis are 10 and 8, respectively. E. Kaplan–Meier survival curve of the DEN-treated WT (n=11) and Cic LKO mice (n=11). All error bars show s.e.m. *P < 0.05.

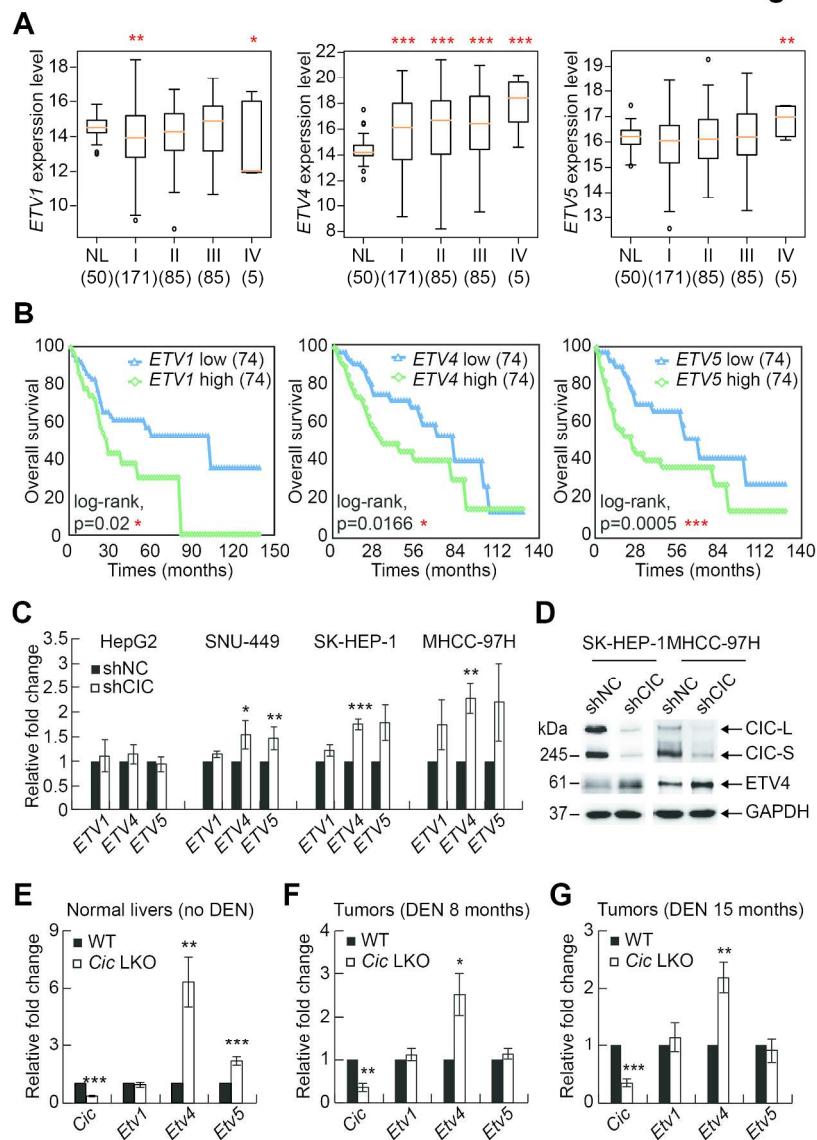203x223mm (300 x 300 DPI)

Fig.5

Figure 5. ETV4 is a major CIC target with the most significant relevance to HCC among PEA3 group genes. A. Analysis of TCGA database for expression levels of ETV1, ETV4, and ETV5 in normal liver (NL) and HCC samples of four different clinicopathologic stages (I, II, III, and IV). The numbers in parentheses mean the number of subjects in each group. B. Kaplan-Meier analysis of overall survival for HCC patients with high or low expression of PEA3 group genes (74 patients per each subgroup). C. qRT-PCR analysis of PEA3 group gene expression levels in control and CIC knockdown HCC cells. Experiments were performed more than three times, independently. D. Western blot analysis for levels of ETV4 in control and CIC knockdown HCC cells. E. qRT-PCR analysis for levels of Cic, Etv1, Etv4, and Etv5 in livers of 7-week-old WT and Cic LKO mice. n=6 per each genotype. F and G. qRT-PCR analysis for levels of Cic, Etv1, Etv4, and Etv5 in liver tumors harvested from the DEN-treated WT and Cic LKO mice at 8 months of age (F) and at 15 months of age (G). n=5 per each genotype. All error bars show s.e.m. *P < 0.05, **P < 0.01, and ***P < 0.001.

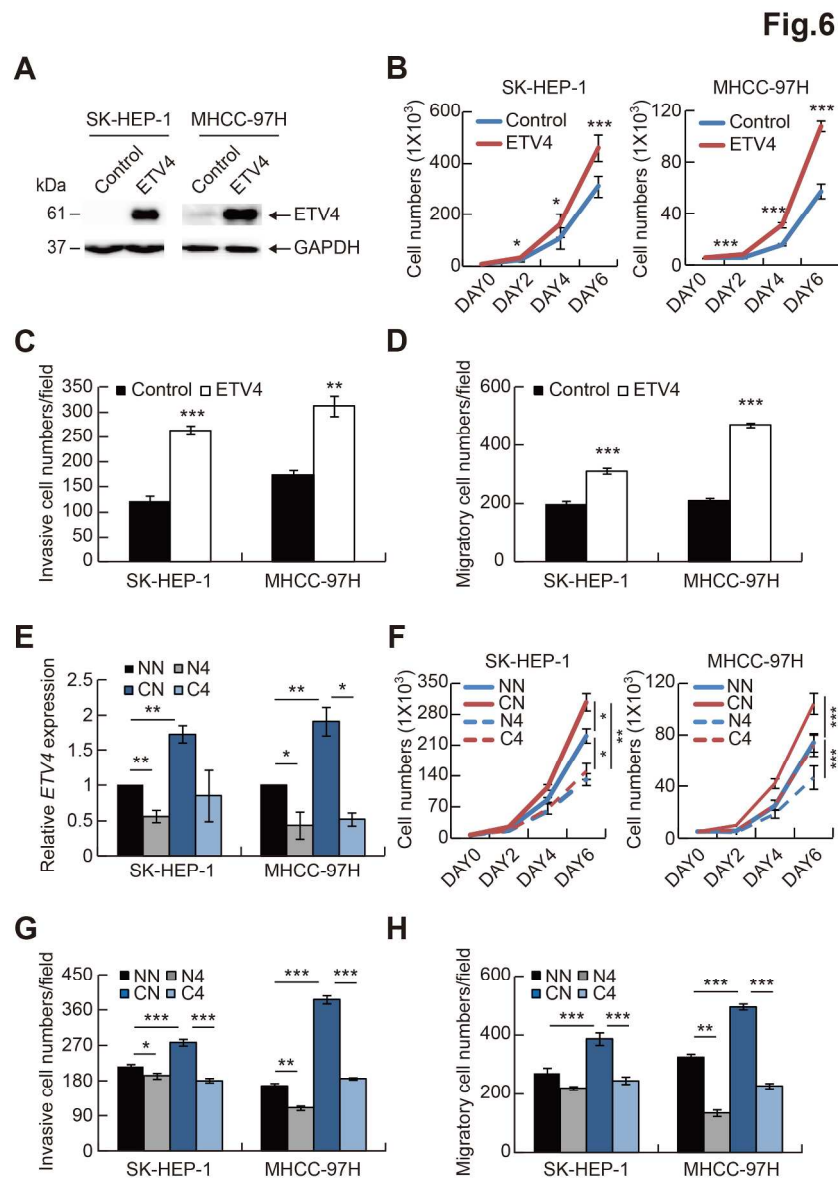204x278mm (300 x 300 DPI)

Fig.6

Figure 6. CIC deficiency-mediated promotion of HCC progression is due to derepression of ETV4. A. Western blot analysis showing ectopic expression of ETV4 in SK-HEP-1 and MHCC-97H cells. B-D. Cell growth assay (B), matrigel invasion assay (C), and transwell migration assay (D) of control and ETV4-overexpressing HCC cells. E. qRT-PCR analysis for ETV4 mRNA levels in control and CIC knockdown HCC cells transfected with either control or ETV4 siRNA. NN: control HCC cells transfected with control siRNA, N4: control HCC cells transfected with ETV4 siRNA (siETV4), CN: CIC knockdown HCC cells transfected with control siRNA, and C4: CIC knockdown HCC cells transfected with siETV4. F-H. Cell growth assay (F), matrigel invasion assay (G), and transwell migration assay (H) of control and CIC knockdown HCC cells treated with either control or ETV4 siRNA. Three independent experiments were performed. All error bars show s.e.m. *P < 0.05, **P < 0.01, and ***P < 0.001.
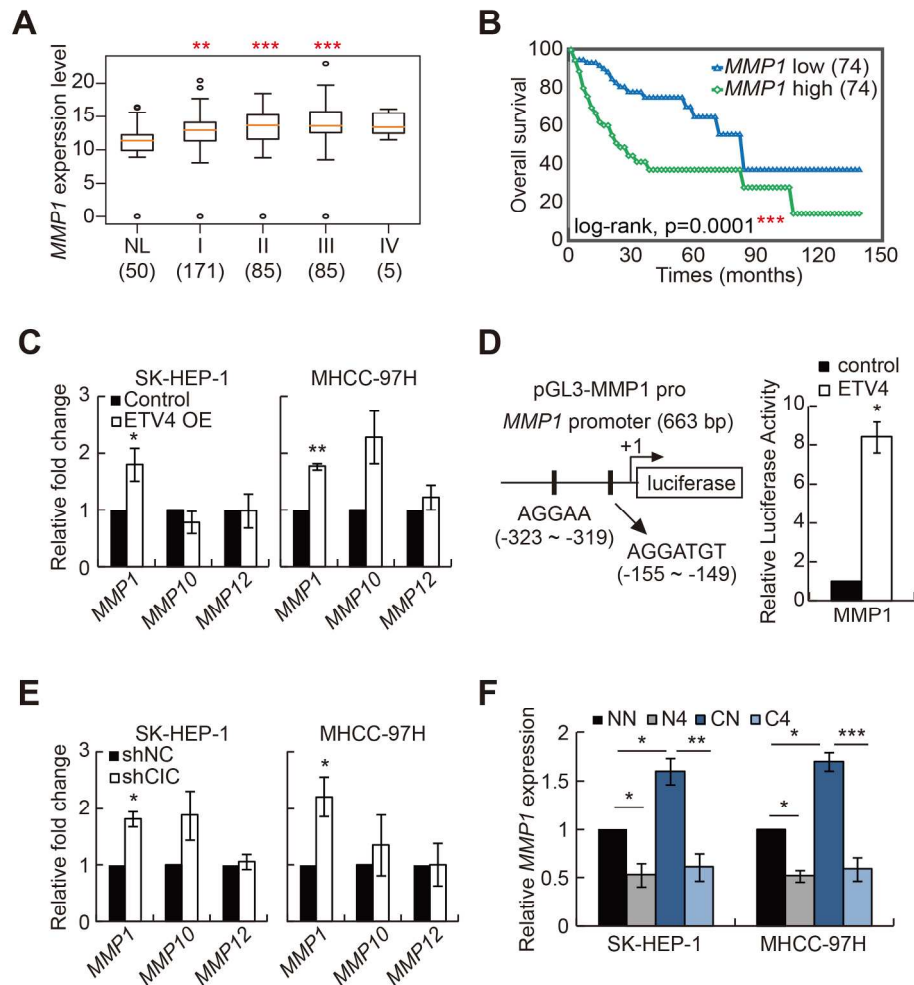
204x271mm (300 x 300 DPI)

Fig.7

Figure 7. MMP1 expression is regulated by the CIC-ETV4 axis. A. Analysis of TCGA database for expression levels of MMP1 in normal liver (NL) and HCC samples of four different clinicopathologic stages (I, II, III, and IV). The numbers in parentheses mean the number of subjects in each group. B. Kaplan-Meier analysis of overall survival for HCC patients with high or low MMP1 expression (74 patients per each subgroup). C. qRT-PCR analysis for levels of MMP1, MMP10, and MMP12 in control and ETV4-overexpressing HCC cells (SK-HEP-1 and MHCC-97H). D. Dual luciferase assay for regulation of MMP1 promoter activity by ETV4. The left panel is a schematic illustration for the luciferase reporter construct harboring MMP1 promoter region (-663/+1), in which there are two putative ETV4 binding sites (-323/-319 and -155/-149). The right panel is a bar graph for relative luciferase activity in the presence or absence of ETV4 overexpression. E. qRT-PCR analysis for levels of MMP1, MMP10, and MMP12 in control and CIC knockdown HCC cells. F. qRT-PCR analysis for MMP1 levels in control and CIC knockdown HCC cells treated with either control or ETV4 siRNA. NN: control HCC cells transfected with control siRNA, N4: control HCC cells transfected with siETV4, CN: CIC knockdown HCC cells transfected with control siRNA, and C4: CIC knockdown HCC cells transfected with siETV4. Three independent experiments were performed. All error bars show s.e.m. *P < 0.05, **P < 0.01, and ***P <
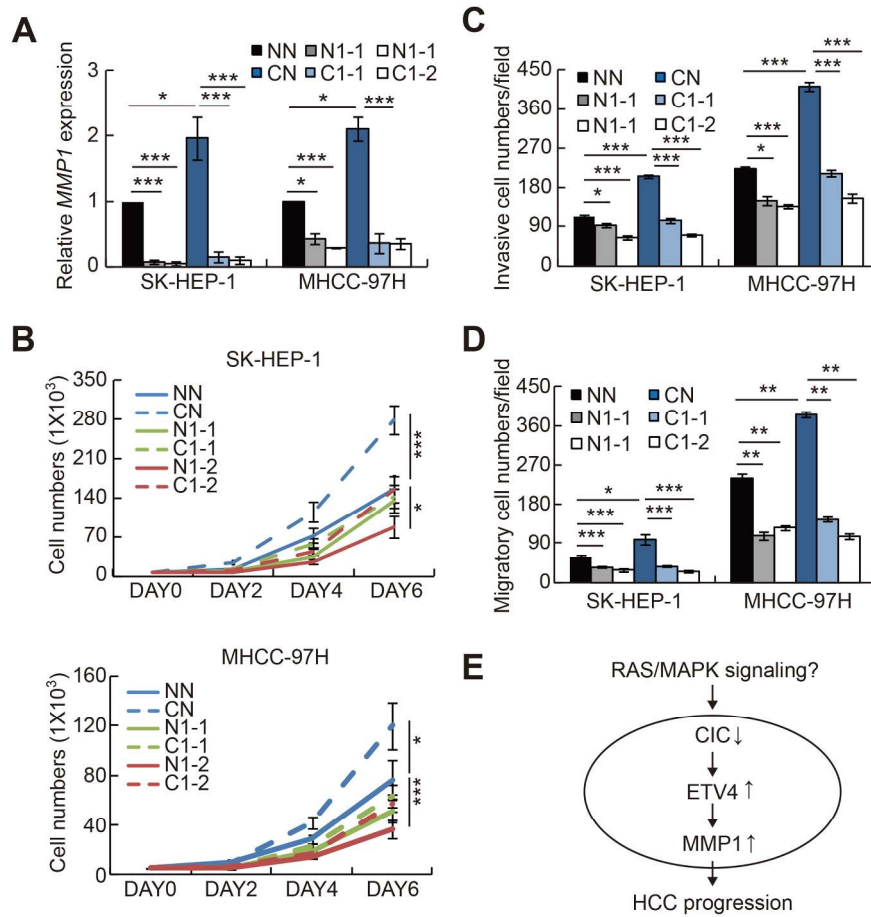
0.001.

205x243mm (300 x 300 DPI)

Fig.8

Figure 8. Upregulation of MMP1 expression contributes to the increased cell proliferation and invasion in CIC knockdown HCC cells. A. qRT-PCR analysis for MMP1 levels in control and CIC knockdown HCC cells treated with either control or MMP1 siRNAs. NN: control HCC cells transfected with control siRNA, N1-1: control HCC cells transfected with MMP1 siRNA-1 (siMMP1-1), N1-2: control HCC cells transfected with MMP1 siRNA-2 (siMMP1-2), CN: CIC knockdown HCC cells transfected with control siRNA, C1-1: CIC knockdown HCC cells transfected with siMMP1-1, and C1-2: CIC knockdown HCC cells transfected with siMMP1-2. B-D. Cell proliferation assay (B), matrigel invasion assay (C), and transwell migration assay (D) of control and CIC knockdown HCC cells treated with either control or MMP1 siRNAs. Three independent experiments were performed. All error bars show s.e.m. *P < 0.05, **P < 0.01, and ***P < 0.001. E. Proposed model for the regulation of HCC progression by CIC-ETV4-MMP1 axis.

202x226mm (300 x 300 DPI)